Osteoarthritis and Cartilage 27 (2019) 1244–1251

Osteoarthritis and Cartilage

Raman Spectroscopy identifies differences in ochronotic and non-ochronotic cartilage; a potential novel technique for monitoring ochronosis

A.M. Taylor † *, D.D. Jenks †, V.D. Kammath †, B.P. Norman ‡, J.P. Dillon ‡, J.A. Gallagher ‡, L.R. Ranganath §, J.G. Kerns †

† *Lancaster Medical School, Faculty of Health & Medicine, Lancaster University, Bailrigg, Lancaster, UK*
‡ *Department of Musculoskeletal Biology, Institute of Ageing and Chronic Disease, University of Liverpool, Liverpool, UK*
§ *Department of Clinical Biochemistry and Metabolic Medicine, Liverpool Clinical Laboratories, Royal Liverpool University Hospital, Liverpool, UK*

ARTICLE INFO

Article history:
Received 24 October 2018
Accepted 10 April 2019

Keywords:
Alkaptonuria
Ochronosis
Arthropathy
Raman spectroscopy
Osteoarthritis
Cartilage

SUMMARY

Objective: Alkaptonuria (AKU) is a rare, inherited disorder of tyrosine metabolism, where patients are unable to breakdown homogentisic acid (HGA), which increases systemically over time. It presents with a clinical triad of features; HGA in urine, ochronosis of collagenous tissues, and the subsequent ochronotic arthritis of these tissues. In recent years the advance in the understanding of the disease and the potential treatment of the disorder looks promising with the data on the efficacy of nitisinone. However, there are limited methods for the detection and monitoring of ochronosis *in vivo*, or for treatment monitoring.
The study aim was to test the hypothesis that Raman spectra would identify a distinct chemical fingerprint for the non-ochronotic, compared to ochronotic cartilage.
Design: Ochronotic and non-ochronotic cartilage from human hips and ears were analysed using Raman spectroscopy.
Results: Non-ochronotic cartilage spectra were similar and reproducible and typical of normal articular cartilage. Conversely, the ochronotic cartilage samples were highly fluorescent and displayed limited or no discernible Raman peaks in the spectra, in stark contrast to their non-ochronotic pairs. Interestingly, a novel peak was observed associated with the polymer of HGA in the ochronotic cartilage that was confirmed by analysis of pigment derived from synthetic HGA.
Conclusion: This technique reveals novel data on the chemical differences in ochronotic compared with non-ochronotic cartilage, these differences are detectable by a technique that is already generating *in vivo* data and demonstrates the first possible procedure to monitor the progression of ochronosis in tissues of patients with AKU.

Introduction

Alkaptonuria (AKU) is a rare autosomal recessive disorder of tyrosine metabolism. The condition affects 1 in 250,000–500,000 people and results from the absence of the enzyme homogentisate 1,2-dioxygenase (HGD). This enzyme undertakes the highly specific process of cleaving the benzene ring of homogentisic acid (HGA) to produce maleylacetoacetate acid[1]. The condition presents with a triad of clinical features; the first and earliest, presenting from birth, is homogentisic aciduria, which darkens on exposure to air, or on addition of alkali. The second is ochronosis of collagenous tissues, such as the pinna, sclera and articular cartilages of weight bearing joints, usually seen in the third decade of life, but it is unclear exactly when this commences. The third and final feature is ochronotic osteoarthropathy, which usually manifests in the fourth decade of life and affects larger weight-bearing joints that have been subject to many years of ochronosis[2]. There is still no

* Address correspondence and reprint requests to: A.M. Taylor, Lancaster Medical School, Furness College, Lancaster University, Bailrigg, Lancaster LA1 4YG, UK. Tel: 441524593131.
E-mail addresses: a.m.taylor@lancaster.ac.uk (A.M. Taylor), d.jenks@lancaster.ac.uk (D.D. Jenks), v.kammath@lancaster.ac.uk (V.D. Kammath), Brendan.Norman@liverpool.ac.uk (B.P. Norman), dillon@liv.ac.uk (J.P. Dillon), jag1@liv.ac.uk (J.A. Gallagher), lrang@liv.ac.uk (L.R. Ranganath), j.kerns@lancaster.ac.uk (J.G. Kerns).

https://doi.org/10.1016/j.joca.2019.04.012
1063-4584/

approved treatment for AKU, but nitisinone has shown excellent capacity for preventing HGA, the causative molecule in the condition, building up[3] and is completely effective at inhibiting ochronosis in AKU mice[4]. A recent study has shown that nitisinone arrests ochronosis and decreases rate of progression of Alkaptonuria in patients[5]. The effectiveness of nitisinone has shown no adverse effects on osteoarticular cells but can cause corneal opacities, which reverse following withdrawal of the drug[6,7].

For patients who have long term established ochronosis the only treatment is joint replacement surgery; however, this shows high variability within a patient and between patients, as not all joints progress to this state at the same rate[8]. The reasons for this are still to be fully understood, but it has been suggested that local inflammation, damage or other factors may contribute[9].

The process of ochronosis in collagenous tissues has been shown to disrupt the molecular/atomic structure of type II collagen[10]. Most recently glycosaminoglycans (GAGs) have been shown to be absent or not extractable from macroscopically ochronotic cartilage[11]. The changes that occur in the extracellular matrix of ochronotic cartilage change both the mechanical and biochemical properties[8]. Whilst there has been an advance in the understanding of AKU, it is still unclear when ochronosis starts and whether the process can be reversed *in vivo*. One of the most accessible and easily observable areas that becomes pigmented is the pinna, which can therefore be used for monitoring ochronosis over time. However, although visual estimates are possible, the most accurate measure of ochronosis is a biopsy, which can be painful and potentially disfiguring.

Raman spectroscopy is a non-destructive technique that provides a chemically specific signature of a given sample. It has a broad range of applications but is used extensively to probe the chemistry of *in vitro* and *ex vivo* human samples from a range of pathologies[12]. Furthermore, in recent years numerous techniques have emerged and been developed that will allow and support *in vivo* measurements[13]. As a laser-based technology it uses a specific monochromatic wavelength to excite molecular bonds in a given sample. Following the molecular vibration, the photons are, either, released at the same energy and wavelength (Rayleigh scattering), or an exchange in energy occurs and the photons released have either lost or gained energy, resulting in a wavelength shift; this is known as Raman scattering, and specific to the energy of the molecular bonds. Therefore, it enables the acquisition of a specific Raman signature or fingerprint of a given material by characterising the chemical bonds within it. Compared to current clinical diagnostic techniques for bone disorders, Raman spectroscopy has some advantages as it can provide information on both the inorganic and organic material present, and is non-ionising[14]. An example of the potential for bone disease diagnosis is osteogenesis imperfecta, a collagen disorder, which can be identified *ex vivo* and *in vivo* using Raman spectroscopy[15]. It has also been used *ex vivo* to identify osteoarthritis[16] and there is some evidence that it may be useful for identifying osteoporosis[13,17,18]. Furthermore, chemical differences have been found with AKU cartilage samples using Fourier transform infrared spectroscopy, a technique complementary to Raman spectroscopy, but which does not lend itself to clinical applications due to its sensitivity to water[20]. The aim of this study is to investigate the chemical composition and potential differences in ochronotic and non-ochronotic cartilage using Raman spectroscopy.

Methods

Materials

Hip cartilage samples

Hip cartilage samples, (n = 3 pairs (pigmented and non-pigmented)) were obtained as surgical waste with informed patient consent following ethical approval by Liverpool REC (07/Q1505/29). The samples were dissected immediately following surgery into ochronotic and non-ochronotic pairs and stored unfixed at −80°C.

Ear cartilage biopsy

Ear biopsy samples (n = 27; aged 16–67 years, 12 males and 15 females, equal males and females within each age group) were obtained, with ethical approval from Preston REC (15/NW/0749), as part of the Subclinical Ochronotic Features In Alkaptonuria (SOFIA) study; patient characteristics given in Table I.

Ear visual ochronosis score

Ear visual ochronosis score was undertaken by a single blinded scorer, this was performed as part of the SOFIA study where pigmentation across both ears of a single patient was measured. Ears were classified into 1 of four groups as having none (0), slight (1), moderate (2) or marked (3) pigmentation. The scores from each ear were combined to give the overall ear visual ochronosis score. We have added a supplementary figure (Suppl. Fig 1) to demonstrate the four groups.

Ear biopsy % ochronosis score

A 4 mm diameter biopsy was taken from the conchal bowl of the ear using a posterior approach under local anaesthetic. A single stitch was used at the end of the ear biopsy. The biopsy was fixed in a 4% solution of formaldehyde in phosphate buffered saline for 48 h and then transferred to a solution of 70% ethanol in water.

Each biopsy contained a disc of cartilage 4 mm in diameter and 1–2 mm thick. The disc was bisected along the diameter and a thin slice of 0.8 mm was taken from the cut face. This sample was examined using an Olympus SZH binocular microscope in darkfield mode at 7.5× magnification. The biopsy section was photographed using a 9M pixels DCM 900 camera and images stored as TIFFS. TIFFs were opened in Image J as 8-bit RGB images. An oval region of

Table I
Table of patient demographics and their visual and biopsy ochronosis scores

SOFIA ID	Age	Gender	Visual ear ochronosis score	Ear biopsy % ochronosis score
3	62	M	2	60
5	59	F	3	4
6	43	M	3	100
7	46	M	6	99.6
8	36	F	1	29
9	57	M	6	59
10	33	M	0	9
11	34	F	2	0
12	46	F	3	58
13	43	F	0	38
14	67	F	6	81
15	29	F	0	20
16	43	F	4	71
17	33	M	0	0
18	49	M	3	20
19	49	M	3	11
20	37	F	0	44
21	35	F	0	11
22	31	F	0	0
23	20	F	0	29
24	16	M	0	0
25	16	M	0	0
26	26	F	0	0
27	24	F	0	0
28	22	M	0	0
29	23	M	0	0
30	23	F	0	0

interest 3 mm long by 1 mm wide was selected and the mean colour intensity in the blue channel was quantified on 255 scale, transformed so that white = 0 and black = 255. Following subtraction of the absorbance of non-ochronotic tissue the % absorbance was calculated (non-ochronotic tissue = 0 and completely ochronotic tissue = 100), which provided an ear biopsy % ochronosis score. Presence of ochronotic pigmentation was confirmed by histology on serial sections followed by Schmorl staining and microscopy (data not shown).

Sample preparation

For analysis via Raman, individual cartilage samples were placed onto an inert calcium fluoride (CaF_2) disc for analysis. Samples were secured using clingfilm, with a hole where measurements were taken, which also ensured the samples did not dry out during spectral acquisition.

Instrumentation

Raman spectra were acquired from the samples using an InVia Raman microspectrometer (Renishaw plc, Gloucestershire, UK), equipped with a 785 nm laser, 200 mW at source, ~10 mW at sample. A minimum of five spectra were collected from each sample, all spectra were acquired in the spectral range 600–1700 cm^{-1}. Spectral resolution was 1 cm^{-1}.

Hip sample spectral acquisition and processing

Spectra were collected over 60 s (20 s × 3 accumulations), at 100% power, from the non-ochronotic tissue. However, applying the same settings to the ochronotic tissue resulted in detector saturation. Therefore, spectra were collected over 10 s (1 s × 10 accumulations), at 100 % power, from the ochronotic tissue. This setting was also tested on the non-ochronotic sample but resulted in spectra with a very low signal to noise (S/N) ratio. Data were baseline corrected, using polynomial (order 5) subtraction, to remove fluorescence and normalised to the phenylalanine peak (1,000 cm^{-1}). A further liquid sample of pure HGA polymer, synthesised in the lab, was analysed with a drop placed on the disk. The polymer was analysed to help identify a characteristic Raman spectrum that might have been present in the tissue samples. Six spectra were acquired at 50% power for 60 s (1 s × 60 accumulations); higher power resulted in detector saturation.

Ear sample spectral acquisition and processing

To acquire spectra from the majority of the samples, i.e., to avoid detector saturation from the highly ochronotic regions, while collecting good quality S/N from the non-ochronotic regions the spectra were collected over 5 s (1s × 5 accumulations) at 50 % power, with cosmic ray removal turned on. Spectra were collected every 200 μm across the longest axis of each sample (samples were ellipsoidal in shape), with a minimum of 15 spectra per sample. 448 spectra were collected in total, 44 were saturated, leaving a total of 404 spectra for analysis.

All spectra were baseline corrected using a fifth order polynomial subtraction and vector normalised using an in-house written Matlab (v2017a, The Mathworks, Inc., Natick, MA, USA) script. Principal component analysis (PCA) and PCA-linear discriminant analysis (PCA-LDA) was then performed on this data. Data were grouped by ear ochronosis and ear pigmentation scores, and by degree of fluorescence in the raw spectra. The latter, with PCA, was used to enable a 'blind' and unsupervised approach to identify natural variation in the Raman spectral data.

A fluorescence to Raman ratio was calculated by comparing the peak height of the raw intensity (counts on *y*-axis) to baselined spectra at 783 cm^{-1}. This peak was chosen as it was consistently present in the spectra and was identified as contributing to differences between non-ochronotic and ochronotic samples from PCA-LDA. As the ochronotic samples were highly fluorescent the area under the curve was calculated for each raw spectrum to provide a measure of the amount of fluorescence.

Results

Hip samples

The average spectrum from each of the non-ochronotic samples is presented in Fig. 1(A); it can be observed by eye that they are similar and reproducible.

Raw spectra acquired from the ochronotic samples are presented in Fig. 1(B); they are remarkably similar to each other. The strongest feature of these spectra is that they reveal a high degree of fluorescence and do not contain easily identifiable peaks that are comparable to either the non-ochronotic cartilage or the cartilage spectra in the literature. Upon baseline correction [Fig. 1(C)] it was possible to identify several peaks, although the quality of the spectra is poor. The main peaks identified were at 626 cm^{-1}, 775 cm^{-1} and 1,675 cm^{-1}.

The synthesised HGA polymer produced similar results to the ochronotic samples, in that the spectra showed high levels of fluorescence and with 100% power resulted in detector saturation. Upon baseline correction [Fig. 1(D)], peaks were identifiable, the largest and most distinct at 1,675 cm^{-1}, with others at 1,072 cm^{-1} and a broad band at 1,310 cm^{-1}.

Ear samples

As with the non-ochronotic spectra from the hip cartilage, the equivalent from the ear samples also provided spectra that had clearly identifiable spectral bands, and a different fluorescence profile to the ochronotic samples, which were highly fluorescent [Fig. 2(A)]. Once processed the Raman spectral profiles were more comparable to non-ochronotic spectral profiles [Fig. 2(B)].

The fluorescence, as determined by the area under the curve, was strongly correlated with both the visual ear ochronosis score (R^2 = 0.73; Fig. 3(A)) and the ear biopsy % ochronosis score (R^2 = 0.63; Fig. 3(B)). Of the samples, one in particular had clearly defined ochronotic and non-ochronotic regions [Fig. 3(C)], the spectral ratio of fluorescence to Raman (raw divided by baseline corrected peak height at 783 cm^{-1}) signal clearly maps onto the image; specifically, regions of high ochronosis have a higher fluorescence to Raman ratio [Fig. 3(D)]. Of note is that the darker regions on the right of the sample [Fig. 3(C)] resulted in spectra that were saturated, so we hypothesise that had they been measurable the fluorescence would have been higher from point 12–16 [Fig. 3(D)].

In a PCA scores plot the closer two scores are to each other the more similar they are spectrally, and therefore biochemically, and vice versa. Fig. 4(A) demonstrates that there is a clear separation in the PCA scores plot between samples classified as non-ochronotic compared to ochronotic. There is some overlap of the 95% confidence intervals, however, this is likely because some of the samples contained regions that were both ochronotic and non-ochronotic, such as the one shown in Fig. 3(C). This is further demonstrated in the PCA-LDA scores plot of the same data [Fig. 4(B)]; this 1D plot shows that the most ochronotic spectrum is furthest to the right. The loadings plot [Fig. 4(C)] reveals that the spectral, and therefore biochemical, reason for the separation is primarily due to variation

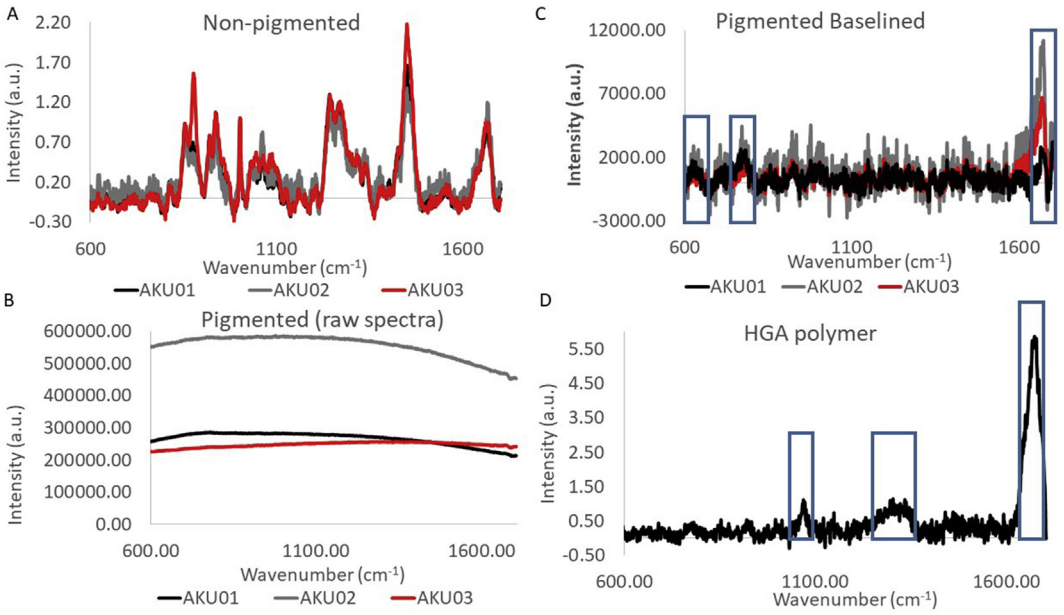

Fig. 1. Raman spectra from ochronotic and non-ochronotic hip cartilage samples from patients with AKU. [A] Average spectrum from each hip sample of non-ochronotic cartilage, baseline corrected and normalised; [B] Average raw spectrum from each sample of ochronotic cartilage; [C] Average spectrum from each sample of ochronotic cartilage, baseline corrected. Blue boxes highlight identifiable peaks; [D] Baseline corrected spectrum of the synthesised homogentisic acid (HGA) polymer. Blue boxes highlight identifiable peaks.

at 783 cm^{-1} (collagen), 879 cm^{-1} (tryptophan/hydroxyproline), 718 cm^{-1} (DNA), 886 cm^{-1} (collagen), 1,199 cm^{-1} (NH_2), 1,657 cm^{-1}(carbonyl; C═O) 1,451 cm^{-1} (CH_2) and 1,333 cm^{-1} (collagen), 1,149 cm^{-1} (NH_2), 976 cm^{-1} (C–H stretch phenylalanine/C–C stretch tryptophan) in order of highest contribution to the variance, to the lowest.

Further analysis [Fig. 4(D)] highlights the spread of individuals' data compared to the data grouped by ochronosis. This not only demonstrates the separation of samples based on ochronosis but also the intra-sample variation, i.e., the heterogeneity of ochronosis within one patient sample.

Analysing the Raman spectra with PCA-LDA according to ear biopsy % ochronosis score demonstrates that the samples without ochronosis are distinct from those with at least 60% ochronosis [Fig. 4(E)]. The samples with varying degrees of ochronosis appear as a spread across both regions but reveal differences within and between samples.

Discussion

This study demonstrates the novel application of Raman to the rare genetic disease AKU, specifically the ability to distinguish clear chemical differences between non-ochronotic and ochronotic cartilage. The ability to demonstrate subtle differences, undetectable by visual methods, using a technique that is already used clinically means that this could be applied to AKU patients *in vivo* for real time monitoring of ochronosis and to determine appropriate time to treat. The spectra from the non-ochronotic samples, hip (hyaline) and ear (elastic) cartilage were comparable to each other and are typical of articular[19] and elastic[21] cartilage spectra, respectively. The main difference is the presence of elastin fibres, and while a direct comparison of the two cartilage types may identify spectral differences, this is not clear from the raw spectra, and no direct comparisons were made. Although the hip spectra were acquired using 1 min spectra, this setting was the optimal for signal to noise ratio and discernible peaks could be identified on smaller collection times, as observed with 5 s ear spectra. Spectra acquired from the ochronotic cartilage from all the samples produced the same comparable spectra, which were inundated by fluorescence. Furthermore, it was only possible to collect spectra using minimal exposure settings; any higher resulted in detector saturation and therefore no recorded measurement. However, upon baseline correction and normalisation, peaks become recognisable. Of these peaks one was also present on the HGA polymer spectra (1,675 cm^{-1}), which is likely due to yellow chromophores, specifically p-quinone[22]. This observation presents some of the first evidence of the existence of a quinone-intermediary in the ochronosis process, the exact structure and binding site of this product is still elusive.

The HGA polymer is chemically similar to melanin, the pigment found in skin[23]. However, as reported in the literature it is possible to acquire distinct spectra from a range of skin types with differing levels of melanin[24]. The intermediate in the tyrosine to melanin pathway is L-dopaquinone, which is chemically similar to benzoquinone, the intermediate in the polymerisation of HGA. While it may have been hypothesised that high levels of melanin may produce the same results that have been measured with ochronotic tissue, this was not the case. This is very likely due to a difference in the chemical environment. Specifically, melanin is found intracellularly, whereas HGA becomes bound to the extracellular matrix in addition to cellular deposition. Therefore, the combination of small chemical differences and the environment likely explain the very different vibrational fingerprints. One particular feature of the HGA is the large degree to which it fluoresces and is Raman active.

Fluorescence occurs when there is an overall increase in energy to all the molecules present in a given sample and is a separate and distinct phenomenon to Raman scattering, which provides molecule-specific information. In the majority of Raman spectroscopy studies the first step after acquisition is to remove the fluorescence to leave behind the pure Raman spectrum, it is then necessary to perform analysis, which, as each spectrum can contain ~1,000 variables, often requires multivariate analysis to identify differences due to the presence of different chemicals, e.g., in disease. Utilising both the fluorescence and Raman information (Fig. 3)

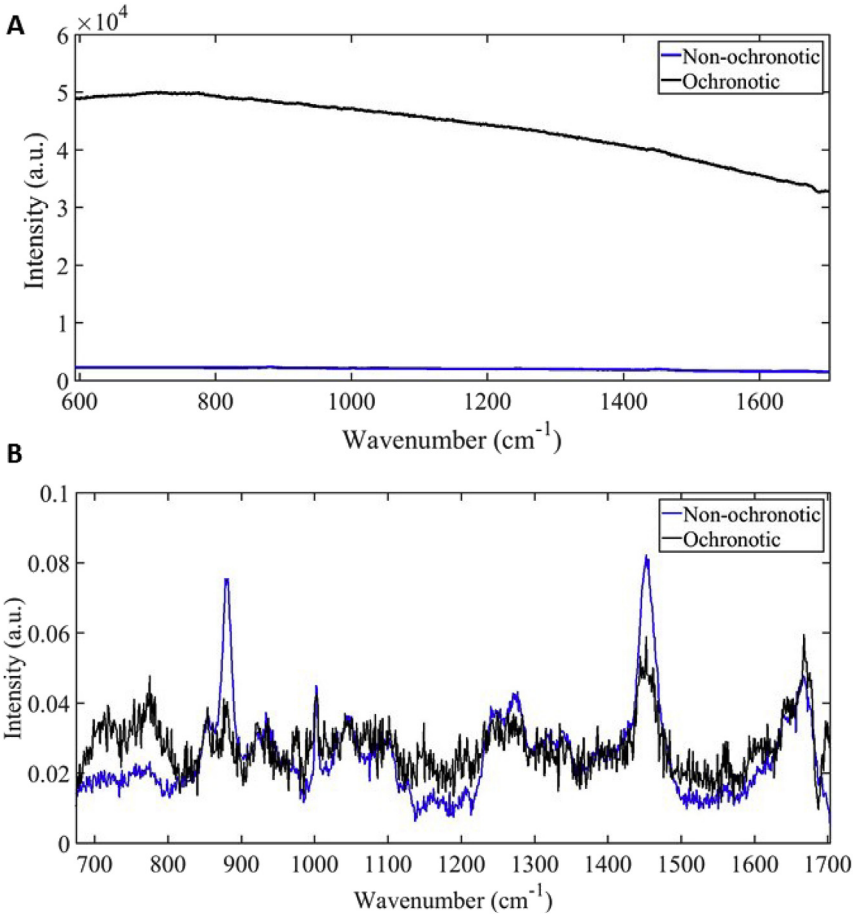

Fig. 2. Raman spectra from ear cartilage samples from patients with AKU. Average spectrum from each class of ear sample: non-ochronotic vs ochronotic cartilage (based on observation of the spectra), [A] raw; [B] baseline corrected and normalised.

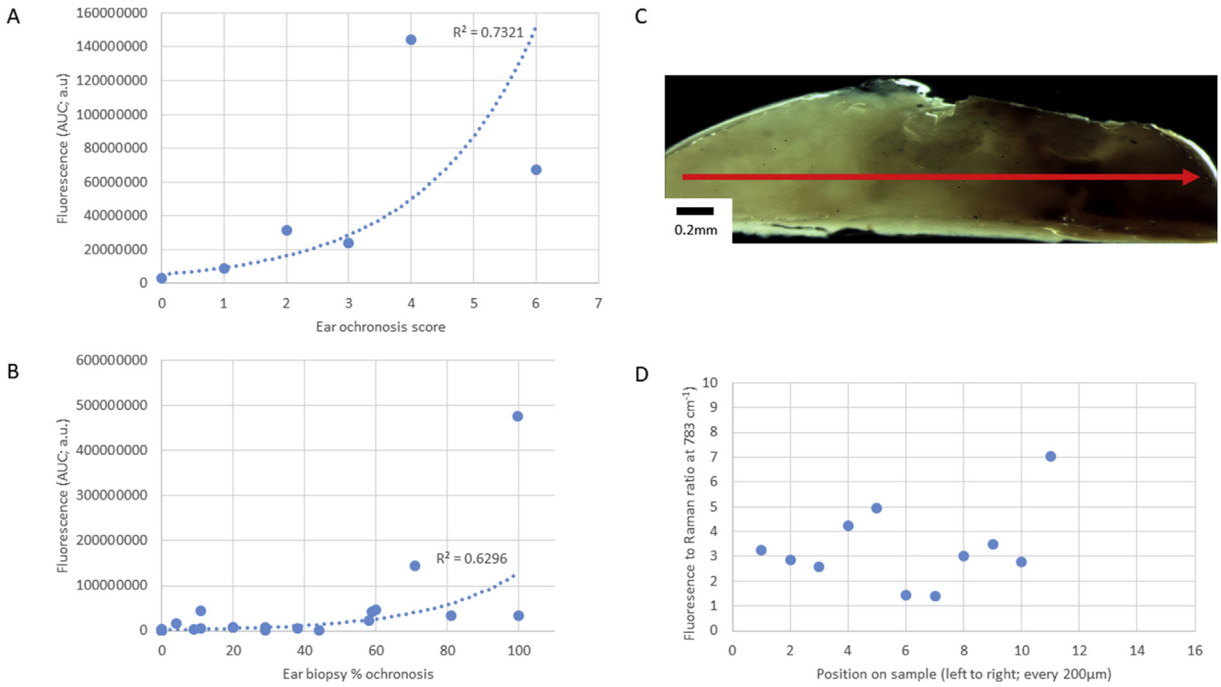

Fig. 3. Comparison of Raman spectroscopy and visual ochronosis assessment in ear cartilage samples from AKU patients. [A] Ear ochronosis score vs fluorescence; [B] biopsy % ochronosis score vs fluorescence; [C] image of an example ear sample with defined ochronotic and non-ochronotic regions, red line is the location Raman spectra were acquired along Spectra were acquired every 200 μm. A scale bar is provided; [D] fluorescence to Raman ratio at 783 cm^{-1} related to position along the sample in [C].

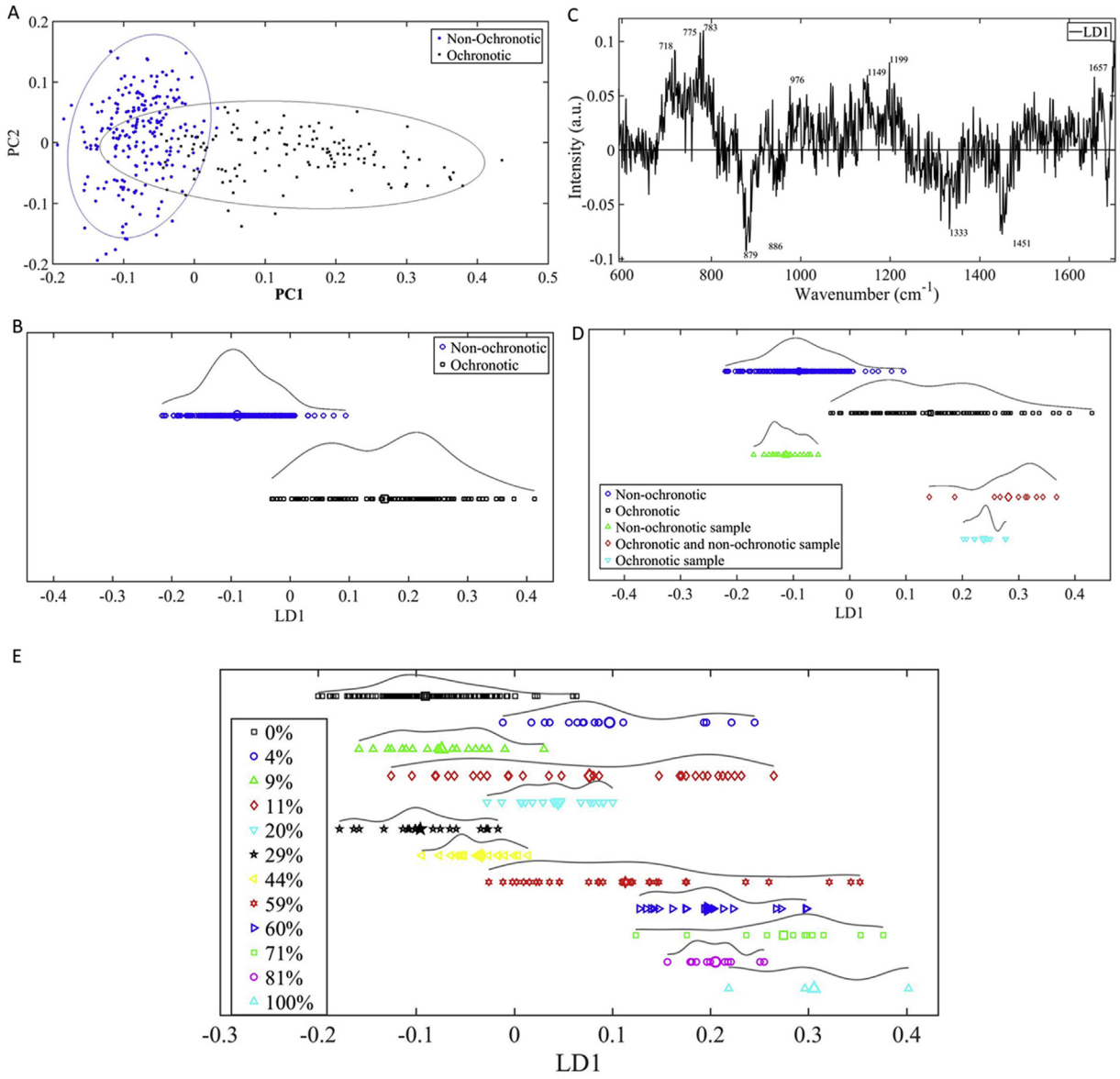

Fig. 4. Principal component analysis (PCA) of Raman spectroscopy distinguishes between ochronotic and non-ochronotic cartilage [A] PCA scores plot of non-ochronotic (blue circles) vs ochronotic (black squares) spectra, with 95% confidence ellipses; [B] PCA-LDA scores plot of non-ochronotic (blue circles) vs ochronotic (black squares) spectra; [C] PCA-LDA loadings plot corresponding to [B], with the labelled peaks showing those that contribute the most; [D] PCA-LDA scores plot of the same data as [B] but with three samples worth of spectra classed individually (non-ochronotic, green triangles; a sample with both ochronotic and ochronotic regions (sample image in Fig. 3(C)) red diamonds; ochronotic sample, blue inverted triangles); [E] PCA-LDA scores plot with the data classed by ear biopsy % ochronosis.

revealed that differences due to ochronosis could be detected. Specifically, there was a strong exponential trend between fluorescence and both the ear ochronosis (visual) and ear biopsy (ear biopsy % ochronosis) scores. Furthermore, the fluorescence to Raman ratio identified that differences within a sample, due to ochronosis, could be observed; the sample in Fig. 3(C) was so pigmented at one side that the detector saturated for the last five spectra. It is assumed that the fluorescence to Raman ratio, had it been measurable, would have been higher here. However, the result of a saturated spectrum is a result in itself as it is strongly associated with high pigmentation.

AKU is a rare disease, and although there is active research, much is still unknown. Although ochronosis is known to occur, the rate and anatomical location varies and is patient-specific. A technique that could monitor pigmentation, to aid in clinical decision making for treatment and in monitoring treatment efficacy would be very valuable. Its most significant use would be the ability to determine the exact time point when an individual should commence nitisinone therapy. This technique has revealed that the presence, or absence, of ochronosis could be identified by measuring fluorescence. Therefore, potentially a visible light source may provide similarly useful information. However, Raman has the added value of providing chemical information. The results shown in Fig. 4 have provided insight into the intra-class, intra-sample and inter-class variation. A comparison of the Raman data to the ear biopsy % ochronosis showed a strong correlation for non-ochronotic and ochronotic cartilage, with overlap in between. This is perhaps expected due to the difference in measurements and the heterogeneous nature of the samples, specifically once ochronosis has started. Furthermore, the biochemical differences between the ochronotic and non-ochronotic samples are due to changes in collagen spectral bands, specifically hydroxyproline,

amide groups and phenylalanine/tryptophan which gives indication as to the association with the pigment and extracellular binding sites, similar to those already identified[10]. Therefore, the technique is providing information about the underlying chemical changes due to the pigmentation, as well as the presence and relative amount of ochronosis.

Overall, the spectra acquired from the non-ochronotic and ochronotic samples are distinctly different at the point of data collection, suggesting that the Raman technique can be used to sensitively detect ochronosis and monitor its progression. Therefore, this has the potential to be a powerful *in vivo* diagnostic tool for AKU. The limitations of this study include a small sampling aperture; future studies would benefit from using an image map analysis approach or a smaller magnification objective, the latter of which may allow a higher power laser to be used. The advantage of this investigation is that although AKU is a rare disease, we were able to collect ear biopsy data from a significant number of participants, and from a range of disease stages. The technique of Raman spectroscopy is already available in a clinical setting to measure bone transcutaneously, albeit in the early trial stages, for osteoporosis[18], osteoarthritis and osteogenesis imperfecta[15]. The technique lends itself to a clinical setting as it benefits from the advantages of being non-invasive and non-ionising, it has also been used to generate distinct spectra from other areas of the body containing connective tissue[25]. The promising benefits of nitisinone for treating AKU is not without its side effects, this technique would enable targeted treatment of patients with this drug by monitoring sites of superficial ochronosis in sites such as the ear, Achilles tendon or patella tendon. Overall, this technique has the potential to be used routinely in clinics for the diagnosis, monitoring and treatment efficacy of individuals with AKU with no adverse health risks.

Author contributions

AMT, JGK, JAG & LRR conceived and designed the study. VDK, DDJ and BN collected samples and undertook data acquisition. JPD processed the ear cartilage biopsies and undertook data acquisition. All authors analysed and interpreted the data, contributed to drafting the manuscript and revising it critically for important intellectual content.

Conflicts of interest

The authors no not have any conflicts of interest.

Funding support

This work was supported by the EU, the Rosetrees Trust, AKU Society, Royal Liverpool University Hospital and the Pathological Society. Ear biopsies were collected as part of the Subclinical Ochronosis Features In Alkaptonuria (SOFIA) a study supported by European Commission Seventh Framework Programme funding granted in 2012 (DevelopAKUre, project number: 304985).

Disclosures

All authors have no disclosures in relation to this manuscript.

Supplementary data

Supplementary data to this article can be found online at https://doi.org/10.1016/j.joca.2019.04.012.

References

1. Mistry JB, Bukhari M, Taylor AM. Alkaptonuria. Rare Dis. 2013 Dec 18;1, e27475.
2. Helliwell TR, Gallagher JA, Ranganath L. Alkaptonuria–a review of surgical and autopsy pathology. Histopathology 2008 Nov;53:503–12.
3. Ranganath LR, Milan AM, Hughes AT, Dutton JJ, Fitzgerald R, Briggs MC, *et al*. Suitability of Nitisinone in Alkaptonuria 1 (SONIA 1): an international, multicentre, randomised, open-label, no-treatment controlled, parallel-group, dose-response study to investigate the effect of once daily nitisinone on 24-h urinary homogentisic acid excretion in patients with alkaptonuria after 4 weeks of treatment. Ann Rheum Dis 2016 Feb;75(2):362–7.
4. Preston AJ, Keenan CM, Sutherland H, Wilson PJ, Wlodarski B, Taylor AM, *et al*. Ochronotic osteoarthropathy in a mouse model of alkaptonuria, and its inhibition by nitisinone. Ann Rheum Dis 2014;73:284–9.
5. Ranganath LR, Khedr M, Milan AM, Davison AS, Hughes AT, Usher JL, *et al*. Nitisinone arrests ochronosis and decreases rate of progression of Alkaptonuria: evaluation of the effect of nitisinone in the United Kingdom National Alkaptonuria Centre. Mol Genet Metabol 2018 Sep;125(1–2):127–34.
6. Mistry JB, Jackson DJ, Bukhari M, Taylor AM. Osteoarticular cells tolerate short-term exposure to nitisinone-implications in alkaptonuria. Clin Rheumatol 2016 Feb;35(2):513–6.
7. Khedr M, Judd S, Briggs MC, Hughes AT, Milan AM, Stewart RMK, *et al*. Asymptomatic corneal keratopathy secondary to hypertyrosinaemia following low dose nitisinone and a literature review of tyrosine keratopathy in alkaptonuria. JIMD Rep 2017;40:31–7.
8. Taylor AM, Boyde A, Wilson PJ, Jarvis JC, Davidson JS, Hunt JA, *et al*. The role of calcified cartilage and subchondral bone in the initiation and progression of ochronotic arthropathy in alkaptonuria. Arthritis Rheum 2011 Dec;63:3887–96.
9. Mistry JB, Jackson DJ, Bukhari M, Taylor AM. A role for interleukins in ochronosis in a chondrocyte in vitro model of alkaptonuria. Clin Rheumatol 2016 Jul;35(7):1849–56.
10. Chow WY, Taylor AM, Reid DG, Gallagher JA, Duer MJ. Collagen atomic scale molecular disorder in ochronotic cartilage from an alkaptonuria patient, observed by solid state NMR. J Inherit Metab Dis 2011 Dec;34:1137–40.
11. Taylor AM, Hsueh MF, Ranganath LR, Gallagher JA, Dillon JP, Huebner JL, *et al*. Cartilage biomarkers in the osteoarthropathy of alkaptonuria reveal low turnover and accelerated ageing. Rheumatology 2017 Jan;56(1):156–64.
12. Butler HJ, Ashton L, Bird B, Cinque G, Curtis K, Dorney J, *et al*. Using Raman spectroscopy to characterize biological materials. Nat Protoc 2016;11:664–87.
13. Matousek P, Draper ERC, Goodship AE, Clark IP, Ronayne KL, Parker AW. Central Laser Facility Annual Report. In: Non-invasive Raman Spectroscopy of Human Tissue in Vivo 2006;vols. 133–135.
14. Morris MD, Mandair GS. Raman assessment of bone quality. Clin Orthop Relat Res 2010;469:2160–9.
15. Buckley K, Kerns JG, Gikas PD, Birch HL, Vinton J, Keen R, *et al*. Measurement of abnormal bone composition in vivo using noninvasive Raman spectroscopy. IBMS BoneKEy 2014;11:602.
16. Kerns JG, Gikas PD, Buckley K, Shepperd A, Birch HL, McCarthy I, *et al*. Evidence from Raman spectroscopy of a putative link between inherent bone matrix chemistry and degenerative joint disease. Arthritis & Rheumatology (Hoboken, N.J.). 2014;66:1237–46.
17. McCreadie BR, Morris MD, Chen TC, Sudhaker Rao D, Finney WF, Widjaja E, *et al*. Bone tissue compositional differences in women with and without osteoporotic fracture. Bone 2016;39:1190–5.

18. Buckley K, Kerns JG, Vinton J, Gikas PD, Smith C, Parker AW, *et al*. Towards the in vivo prediction of fragility fractures with Raman spectroscopy. J Raman Spectrosc 2015;46:610–8.
19. Esmonde-White K. Raman spectroscopy of soft musculoskeletal tissues. Appl Spectrosc 2014;68:1203–18.
20. Mitri E, Millucci L, Merolle L, Bernardini G, Vaccari L, Gianoncelli A, *et al*. A new light on Alkaptonuria: a Fourier-transform infrared microscopy (FTIRM) and low energy X-ray fluorescence (LEXRF) microscopy correlative study on a rare disease. Biochim Biophys Acta Gen Subj 2017;1861:1000–8.
21. Green E, Ellis R, Winlove P. The molecular structure and physical properties of elastin fibers as revealed by Raman microspectroscopy. Biopolymers 2008;89:931–40.
22. Agarwal UP. Assignment of the photoyellowing-related 1675 cm^{-1} Raman/IR band to P-quinones and its implications to the mechanism of color reversion in mechanical pulps. J Wood Chem Technol 1998;18:381–402.
23. Roberts NB, Curtis SA, Milan AM, Ranganath LR. The pigment in alkaptonuria relationship to melanin and other coloured substances: a review of metabolism, composition and chemical analysis. JIMD Rep 2015;24:51–66.
24. Huang Z, Lui H, Chen XK, Alajlan A, McLean DI, Zeng H. Raman spectroscopy of in vivo cutaneous melanin. J Biomed Opt 2004;9:1198.
25. Pudney PD, Bonnist EYM, Caspers PJ, Gorce JP, Marriot C, Puppels GJ, *et al*. A new in vivo Raman probe for enhanced applicability to the body. Appl Spectrosc 2012;66:882–91.